Construction and Building Materials 47 (2013) 888–895

Contents lists available at SciVerse ScienceDirect

Construction and Building Materials

journal homepage: www.elsevier.com/locate/conbuildmat

# Experimental investigation and monitoring of a polypropylene-based fiber reinforced concrete road pavement

A. Nobili [a], L. Lanzoni [a,b,*], A.M. Tarantino [a]

[a] DIMeC – Department of Mechanical and Civil Engineering, University of Modena and Reggio Emilia, Via Vignolese 905, 41125 Modena, Italy
[b] Department of Economy and Technology, University of San Marino, Salita alla Rocca 44, Republic of San Marino 47890, San Marino

## HIGHLIGHTS

- We present the results of an experimental monitoring of a PFRC road pavement.
- The monitoring allows to evaluate the performances of the road structure in time.
- The realized monitoring encompasses both acoustic and strain measurements.
- The ACT results reveal a stable condition of the PFRC road pavement.
- The ACT results were confirmed by the real time acquisition through 12 string gauges.

## ARTICLE INFO

*Article history:*
Received 9 November 2012
Received in revised form 16 April 2013
Accepted 4 May 2013
Available online 19 June 2013

*Keywords:*
Reinforced concrete
Polypropylene fibers
Concrete road pavements
Acoustic measurements
Strain measurements

## ABSTRACT

In this work, basic guidelines are provided for the design of a polypropylene-based fiber reinforced concrete (PFRC) road pavement, as applied in an actual testing section resting inside a tunnel of the "Quadrilatero Marche-Umbria" road empowerment project, Italy. Results of a six-month monitoring carried out on actual traffic loads are also presented, as a feedback to the designing stage. Monitoring encompasses direct measurement of the strain level inside the cast as well as acoustic measurement. It is shown that the fiber reinforced concrete technology provides an efficient, safe as well as cost-effective design solution for roadways, especially inside tunnels.



## 1. Introduction

A rigid road pavement consists of a top concrete pavement resting on underlying courses, usually a base course and an optional sub-base layer. Several important advantages are connected to adopting rigid roadways as opposed to conventional flexible pavements. In particular, a rigid road pavement provides an efficient, comfortable, high-performance and cost effective design choice when dealing with roadways and highways subjected to heavy traffic loads. Indeed, owing to its high flexural stiffness and mechanical resistance, a rigid pavement allows to homogeneously transfer the vehicular loads to the underlying layers, preventing load and stress concentrations in the subgrade and, in turn, deflection and subsidence of the pavement structure (e.g. [1,2]). Moreover, through proper roughening and marking techniques, usually based on suitable floor grinders, micro and macro-texture and, in turn, friction and adherence performance (skid resistance) of the pavement surface may be accurately controlled, which is a key issue in warranting proper safety standards.

The light reflectance property of Portland cement makes the concrete rigid pavement an optimal technology to guarantee suitable illumination standard at a reasonable main power cost [3]. This issue is especially important in tunnel roadways at daytime, owing to the blinding effect of sunlight. Furthermore, concrete pavement may be recycled and reused during maintenance operations and at the servicing life end. On the overall, concrete represents an attractive energy-saving as well as eco-friendly road material.

On the other hand, concrete pavements may undergo rapid deterioration, in the form of micro and macro cracks, fractures and failures, which can cause loss of serviceability and unsafe driving condition. This occurrence is mainly due to the brittle behavior of cement concrete together with its low resistance to fatigue phenomena and its small toughness. However, these detrimental

* Corresponding author at: Department of Economy and Technology, University of San Marino, Salita alla Rocca 44, Republic of San Marino 47890, San Marino.
*E-mail address:* luca.lanzoni@unimo.it (L. Lanzoni).

0950-0618 
http://dx.doi.org/10.1016/j.conbuildmat.2013.05.077

aspects can be mitigated through the adoption of fibers. Indeed, dispersed structural fibers can be added at the mixing stage of concrete in the so-called fiber reinforced concrete (FRC). Many studies have been performed in the last decades concerning the mechanical performance of FRC. It appears that fibers can significantly improve durability, tensile strength and toughness of the cement matrix, preventing the crack opening and growth in concrete members [4] and cementitious composites, like cement-treated road materials [5]. Recently, most attention has been devoted to the adoption of polymeric fibers, because of their advantages over the metallic ones with special regard to chemical stability, lightness and workability. It should be noted that a FRC road pavement may be realized through substantially conventional paving techniques provided some basic guidelines are followed, as explained in this paper. Furthermore, due to their low flexural stiffness, synthetic fibers are especially suitable in the ejected concrete technology (spritz-beton), which takes a great part in the lining construction for tunnels. In addition, polymeric fibers, particularly the polypropylene-based fibers, are proved to improve the fire resistance of concrete, in what is often named the anti-spalling effect. Indeed, even if cement concrete is known as a noncombustible material and no self-propagating fire, it is prone to a pop-up like damaging phenomenon if subjected to high thermal loads. This is especially the case for high resistance concrete (HRC) and silicate added concrete. Under high temperature, polypropylene-based fibers sublimate, thus decreasing the water pressure inside the pores of the cement matrix and preventing crack and expulsion of the outermost layers [6,7]. This makes the FRC a promising technology to realize roadway inside tunnels and galleries, where high safety standards as regard to fire protection are mandatory.

As a result, polypropylene-based fiber reinforced concrete (PFRC) appears to be, besides an appealing building material, a very attractive rigid pavement matrix, with special regard to high-performance and safety.

The present work provides some basic guidelines for designing rigid PFRC pavements, as applied to the design of an actual application. Such application concerns a test pavement within the Italian road network empowerment named "Quadrilatero Marche-Umbria", as a first step to deploy this technology to the whole network.

## 2. Project characteristics

The backbone of the road network empowerment consists of two, almost parallel laneways, one connecting Foligno to Civitanova and the other connecting Perugia to Ancona. A third interconnecting roadway is designed in correspondence of Fabriano and Muccia (see Fig. 1). The road system develops along 160 km, and encompasses several road substructures like secondary roads, road bridges, intersections, roundabouts and 11 tunnels. The project is aimed at connecting the industrial areas in the region, sustaining new business activities and production centers about the road network. Work start took place in 2010 and it is still in due course to date.

In this framework, the paper presents the outcome of a six-month monitoring of the test road, as a mean to provide feedback on the designing stage as well as on the technology.

The pavement under testing is a portion of the Foligno-Civitanova laneway, near Polverina di Camerino (MC), inside the gallery named "Le Fratte", near "Caccamo" lake.

### 2.1. Layout of the road pavement

The rigid pavement structural layout is reported in the present section. The rigid pavement consists of a 25 cm thick PFRC slab, founded onto two layers of differently graded, properly compacted, crushed stone, as reported in Table 1. Such foundation provides the pavement with a rigid support, thus warranting the concrete slab

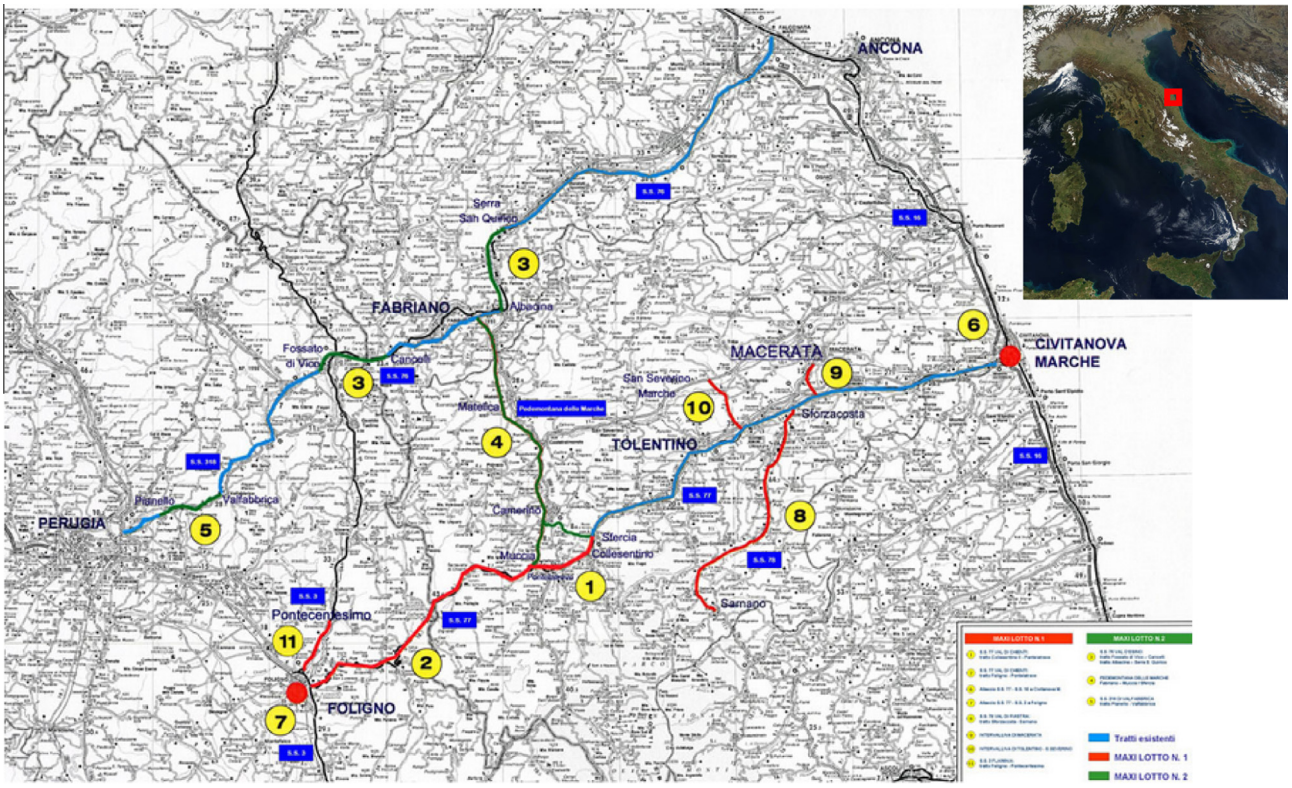


**Fig. 1.** A map of the Italian road network named "Quadrilatero Marche-Umbria".

**Table 1**
Layout of the road pavement.

| Layer | Thickness (mm) | Young modulus (mean) (MPa) |
|---|---|---|
| PHFRC | 250 | 31 000 |
| High quality graded crushed stone | 300 | 400 |
| Crushed stone | 500 | 300 |

good performance in terms of stability and strength. Indeed, the presence of graded crushed stone endowed with high permeability lends the pavement an effective draining capability.

The pavement is provided with a microtexture through transverse grooving obtained through a wire comb.

The tines shall are randomly spaced at roughly 20 mm with no more than 50% of the spacing exceeding 25 mm. A 100 mm to 150 mm wide strip of pavement surface is not tined for the length of each transverse joint, providing an untined surface centered over the transverse joint.

A macrotexture is also imparted through suitably chosen fine aggregates, which enables efficient fluid drainage from the surface.

### 2.2. Composition of the design mixture

The mix design as at Table 2 has been adopted for the rigid road pavement (cement is denominated according to UNI EN 197-1:2011 [23] and aggregates according to UNI EN 12620:2008 [24] specifications).

The mixture is added with polypropylene-based fibers with a length of 39 mm and an equivalent diameter of 0.78 mm, similar to the types A–C fibers reported in [8] (see Fig. 2), at a dosage of 3.5 kg/m$^3$. Polypropylene fibers are added to the concrete mixture at the mixing stage.

The design mixture was chosen for it proved well suited to the adoption of polypropylene-based fibers at the indicated dosage. In turn, polypropylene-based fibers have been selected in light of their cost-effectiveness in terms of performance and applicability. Indeed, an experimental investigation of the mechanical behavior of a PFRC reinforced with the polypropylene-based draw-wire fibers herein employed has been recently carried out and the results are shown in [8].

### 2.3. Transverse joint design

The road pavement is provided with 10 m mutually spaced transverse (with respect the traffic flow) joints, together with an all-along longitudinal joint at the road pavement midwidth. Transverse joints are sawed after a short curing period of the concrete through a conventional early-age sawing technique. Conversely, the longitudinal joint is a construction joint, i.e. it is realized through different casts. The evaluation of the strain level due to hygrometric and plastic shrinkage of the concrete is needed in order to evaluate the proper width of the transverse joints.

According to the Italian technical specifications [17] and disregarding the friction between the pavement and the subgrade layer, the total strain $\varepsilon_{cs}$ due to the shrinkage phenomenon is given as follows:

$$\varepsilon_{cs} = \varepsilon_{cd} + \varepsilon_{ca}; \quad (1)$$

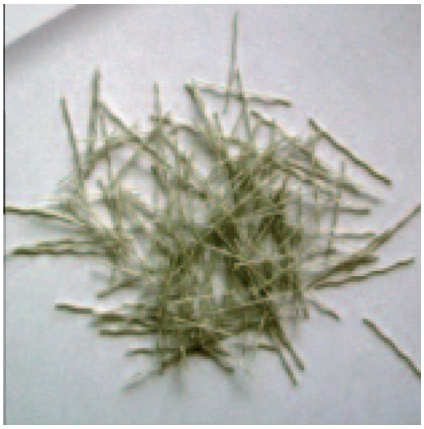

**Fig. 2.** The polypropylene fibers adopted for reinforcing the concrete pavement.

**Table 3**
Values for $\varepsilon_{c0}$.

| $f_{ck}$ | Concrete drying shrinkage | | | | | |
|---|---|---|---|---|---|---|
| | Humidity | | | | | |
| | 20% | 40% | 60% | 80% | 90% | 100% |
| 20 | −0.62 | −0.58 | −0.49 | −0.30 | −0.17 | 0.00 |
| 40 | −0.48 | −0.46 | −0.38 | −0.24 | −0.13 | 0.00 |
| 60 | −0.38 | −0.36 | −0.30 | −0.19 | −0.10 | 0.00 |
| 80 | −0.30 | −0.28 | −0.24 | −0.15 | −0.07 | 0.00 |

**Table 4**
Values for $k_h$.

| $h_0$ (mm) | $k_h$ |
|---|---|
| 100 | 1.0 |
| 200 | 0.85 |
| 300 | 0.75 |
| ⩾500 | 0.70 |

being $\varepsilon_{cd}$ and $\varepsilon_{ca}$ the strain amount due to, respectively, the drying and autogenous concrete shrinkage.

The mean value of the concrete drying shrinkage $\varepsilon_{cd}$ at indefinite time can be evaluated by taking into account the humidity of the environment hosting the concrete pavement and the cylinder compressive strength of the concrete $f_{ck}$, according to Eq. (2) and Tables 3 and 4:

$$\varepsilon_{cd} = k_h \varepsilon_{c0}; \quad (2)$$

being $h_0 = 2Ac/u$; Ac and $u$ denote the pavement cross section and air contact perimeter, respectively.

The mean value long time autogeneous strain rate $\varepsilon_{ca}$ can be evaluated as follows:

$$\varepsilon_{ca} = -2.5(f_{ck} - 10)10^{-6}. \quad (3)$$

**Table 2**
Composition of the mixture.

| Cement | | Aggregates | | | | Fiber | Water/cement ratio |
|---|---|---|---|---|---|---|---|
| Type | kg/m$^3$ | 0/3 kg/m$^3$ | 3/5 kg/m$^3$ | 5/10 kg/m$^3$ | 10/25 kg/m$^3$ | kg/m$^3$ | |
| CEM II/A-L 42.5 R | 340 | 935 | 65 | 400 | 565 | 3.5 | 0.44 |

**Fig. 3.** Transverse (left) and longitudinal (right) joints.

The cylinder compressive strength of the concrete adopted in the cast equals $f_{ck}$ = 30.7 MPa, corresponding to a cube resistance of about 37 MPa.

Here, Ac = 2.2875 m$^2$, $u$ = 9.15 m, resulting in $h_0$ = 0.25 m and $k_h$ = 0.8. The average humidity in the test tunnel was 80%, at which value it is $\varepsilon_{c0} = -0.27‰$ and $\varepsilon_{cd} = -0.216‰$, whereas $\varepsilon_{ca}$ equals $-0.05‰$. By adding these strain rates, it results a mean values of the total longitudinal shrinkage strain of about $-0.266‰$, which corresponds to a joint width of about 3 mm. Transverse joints are reinforced with 50 cm long steel bars, having a diameter of 25 mm and 25 cm wide equally spaced, placed at the pavement mid-plane. The longitudinal joint is 8 mm width and it is reinforced with 80 cm long steel bars having a diameter of 25 mm, 165 cm wide spaced.

Free-movement transverse and longitudinal joints have been adopted for the road pavement. This kind of joint allows the pavement segments to freely move along the longitudinal direction, for only shearing forces are transmitted by the joints. Note that the joint width here considered is consistent with the recommendations of the concrete society [18]. Fig. 3 shows the placing of the transverse joints. After sawing and cleaning, a bituminous sealer was applied to the longitudinal and transverse pavement joints.

## 3. Estimated service life

The pavement service life is assessed following the classic South African Mechanistic Design Method (SAMDM), which takes into consideration the estimated traffic load as well as the climatic conditions together with the aging effects due to fatigue phenomena affecting the mechanical parameters of the structure [9,10].

As well known, the life of a road pavement can be suitably expressed in terms of conventional Equivalent Single Axle Loads (ESALs). Indeed, as suggested by AASHTO specifications and many pavement design manuals, the design pavement life is expressed in terms of the number of 80 kN axle loads which the pavement is able to sustain without a significant loss of carrying capacity. Nevertheless, it is often the case that the actual levels of the axle loads frequently exceed this conventional value (e.g. [11]).

Thus, for sake of precaution, and in order to account for the effect of exceptional loads as well as of the dynamical effect of the traffic flow, in the present analysis an axle load of 240 kN has been adopted to evaluate strain and stress level within the pavement structure. A 800 kPa internal tire pressure, which determines the tire-pavement contact area, has been assumed in the analysis. A 20 mm failure-rut depth has been taken for the subgrade.

Standard elastic analysis provides a peak tensile stress at the lower surface of the pavement equal to 1.895 MPa.

Based on experimental data, the fiber manufacturer claims for concrete reinforced with 3.5 kg/m$^3$ of polypropylene fibers a first flexural strength of 3.5 MPa, such that flexural strength over the maximum tensile stress ratio equals 0.54. This allows assessing the working life of the road pavement by means of an appropriate fatigue law for the PFRC under flexural stress conditions.

In this respect, although several studies concerning the fatigue strength of plain, high-performance and fiber-reinforced concrete under different loading conditions may be found in literature (e.g. [12–16]); none seems to provide a performance decaying law for PFRC.

In the present study, in order to assess the working life of the road pavement, the fatigue law proposed by Mailhot et al. [14] for concrete slabs reinforced with a low (0.5% in volume) dosage of metallic fibers has been assumed:

$$S = 101 - 5.97 \log N; \tag{4}$$

where $S$ denotes the ultimate normal stress as a percent of the static normal limit stress and $N$ represents the number of loading cycles.

Letting $S$ = 0.54 in Eq. (4), one finds that $N$ = 40 million cycles, which, on the basis of a traffic estimated load of 1.3 million equivalent axles per year, amounts to more than a 30 year long service life. This estimate may be considered an acceptable service life prediction for the road pavement under consideration.

## 4. Experimental program and method

The test road pavement has been subjected to time-discrete acoustic wave emission monitoring by means of a portable Acoustic Concrete Tester (ACT) as well as to continuous real-time strain monitoring by means of 12 vibrating-string sensors lodged within the structure of the pavement at the cast time.

### 4.1. Acoustic monitoring

ACTs are widely employed within the modern monitoring techniques [19]. In particular, such devices can be effectively adopted to control damaging phenomena like crack formation and growth, hidden failure and wearing processes affecting the concrete structures. Acoustic measurement consists of evaluating the travelling time of ultrasonic longitudinal wave pulses (ranging between 20 kHz and 1000 MHz) between an emitting transducer and a second receiving detector (transit time). Transit times may be related through specific experimental curves to an indirect measure of some mechanical properties, like Young modulus. In the same fashion, crack formation, surface discontinuities, fracture growth and other failing processes like aging, loss of stiffness etc. result in an increase of the transit time of the propagating waves. Thus, differently from other invasive detecting techniques, time-repeated acoustic measurements may detect the onset of important damaging phenomena without altering the monitored system. Transit time is usually expressed in μs.

In the present study, the acoustic measurements through the ACT have been carried out onto a grid of 6 × 3 points on the surface pavement, the grid points being equi-spaced, extending mainly in the transverse direction (6 points side) and located across the marching lane, which is usually mostly loaded. The grid step length equals 30 cm (see Fig. 4).

The measurements have been performed according to the UNI EN 12504-4 and ASTM C597 specifications [20,21]. In particular, in order to assure an efficient reading on a uneven surface, an elastomeric layer has been interposed in between the detector/emitter and the pavement, thus assuring an extended contact area. Acoustic measurement are necessarily obtained at indirect transmission (cf. UNI EN 12504-4). The revealed transit times are reported in Section 5.2.

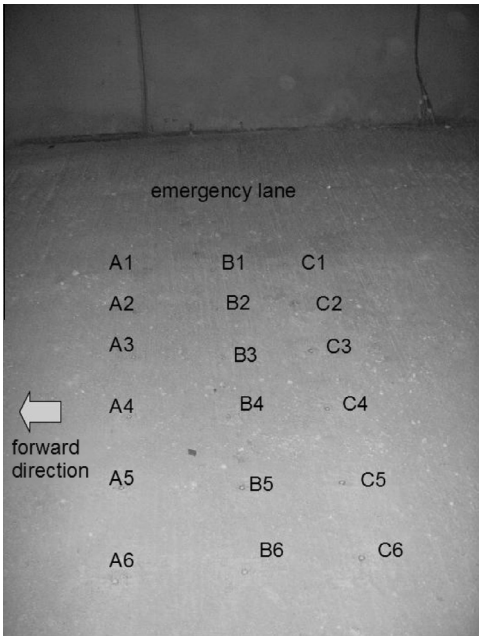


**Fig. 4.** Measuring grid on the marching lane of the pavement subjected to acoustic measurements.

*4.2. Vibrating-string strain monitoring*

The pavement is also endowed with an array of 12 vibrating string strain sensors, placed in near correspondence to the points of the acoustic grid, though far enough to avoid interference. A sun powered data logger collects the strain gauges terminals and periodically transmits the reading (real time acquisition) through the GSM system (see Fig. 5).

Out of this set of strain sensors, six arc weldable sensors (labelled ARC) have been welded to the steel dowel bars of the transverse joint, near the edge of the roadway, where important stress levels are expected due to the boundary effect. The dowels are important to guarantee a proper load transfer across the joints, assuring an efficient collaboration of the portion of the road pavement. Sensor numbering runs from right to left when traveling along the lane.

The other six strain sensors are embedded inside the pavement at the cast stage (labelled CLS). They are placed in three equi-spaced pairs, one gauge measuring longitudinal, the other gauge measuring transverse strain. They are set 3 meters ahead of the arc-weldable sensors (see Figs. 6 and 7).

Sensor numbering again runs from right to left when traveling along the lane, odd (even) numbers standing for longitudinal (transverse) sensors.

Each strain gauge is coupled with a bi-material thermostat in order to provide a temperature compensated reading as well as some information on the climatic conditions.

All the sensors were effectively placed and working after the casting and finishing stage of the pavement, with the exception of one thermostat whose reading could not be obtained. Nonetheless, the relevant strain data appear consistent with the other's and therefore thermally corrected.

Recorded data in terms of temperature and strain levels are reported in Section 5.2.

**Fig. 5.** Wall-mounted data logger powered by the solar panel placed outside the tunnel.

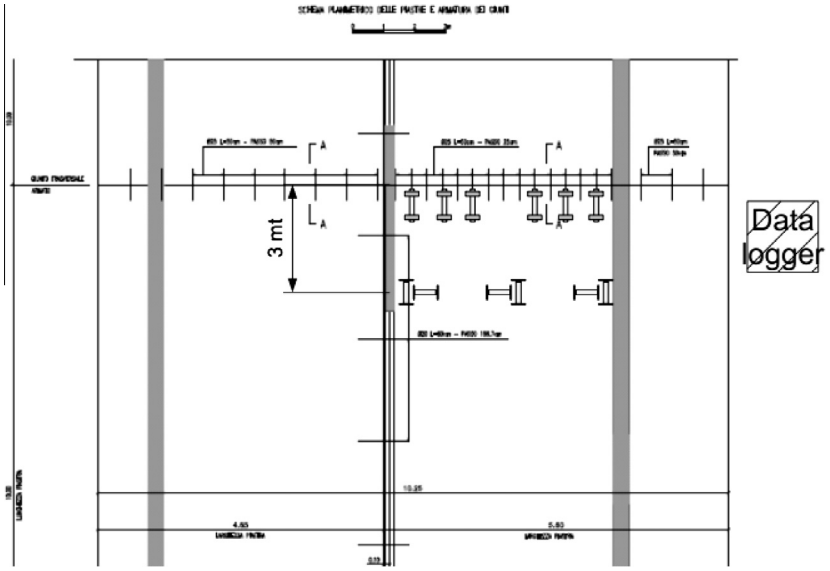


**Fig. 6.** Placement schematic for both embedded and arc-weldable sensors monitoring the road pavement.

**Fig. 7.** (a) Arc weldable sensors (ARC) fixed to the metallic bar in correspondence of the transverse joints and (b) embedded strain gauges (CLS) to be set within the pavement. Sensor numbering runs from right to left when traveling along the lane.

## 5. Experimental results

### 5.1. Crash test

In order to characterize the mechanical resistance of the PFRC employed in the road pavement, and to correlate the concrete compressive strength to the transit time of ultrasonic wave pulses, some samples of fresh mixture have been taken at the cast stage, cured and tested. In particular, 6 $150 \times 150 \times 150$ mm$^3$ cubic samples have been acoustically tested and later crashed in a compressive testing machine after a curing period of 28 days according to UNI EN 12390-3 specification [22] (see Table 5). Crash strength could be thus correlated to the transit time.

### 5.2. Acoustic measurements

Acoustic monitoring was extended for about 4 months, specifically from November 3rd, 2009 to July 23th 2010. Five measurements are here reported. Note that for each measurement, the time of wave propagation between points placed at one and two grid step lengths (30 cm and 60 cm) has been measured in both the transverse and the longitudinal directions. The propagation time between neighboring points (30 cm) is deemed to estimate crack formation inside the depth of the pavement, whereas time of propagation between 60 cm spaced points is connected to the damaging phenomena occurring at the supporting layers.

The set of transverse transit times is reported in Fig. 8. It is observed that beginning on April 15th 2010, single spaced transit times become more scattered, although the average is roughly unchanging. Although difficult to determine, the reason for the significant increase of the transit times recorded on April 15th 2010 may be traced to a settlement of the supporting layer, as suggested by the double spaced transit times, Fig. 8b. It should be observed that double spaced transit times are much more sensitive to experimental errors. It would appear that the supporting layer has undergone a significant compaction (traffic started right after the first measurement date), followed by some performance decay which may be related to the heavy rain conditions encountered in the late spring of 2010.

Longitudinal measurements are presented in Fig. 9. Single spaced measures seem to follow a pattern similar to that encountered for longitudinal data. Likewise, double spaced data hint a stiffness loss in the foundation.

**Table 5**
Compressive resistance of cubic samples of hardened PFRC and transit time.

| Sample | 28 days ultimate load (kN) | Ultimate strength (MPa) | Propagation time of acoustic waves (μs) |
|---|---|---|---|
| 1A | 1003 | 38.0 | 66 |
| 1B | 988 | 39.5 | 69 |
| 2A | 1064 | 37.5 | 55 |
| 2B | 1100 | 38.5 | 54 |
| 3A | 1045 | 37.5 | 66 |
| 3B | 1014 | 38.5 | 66 |

### 5.3. Strain measurements

Real-time continuous monitoring of the strain and thermal fields within the rigid pavement and transverse joint dowels has been carried out through a set of 12 vibrating string temperature compensated gauges. In particular, the strain may be related to the raw frequency data through the following expression given by the sensor manufacturer:

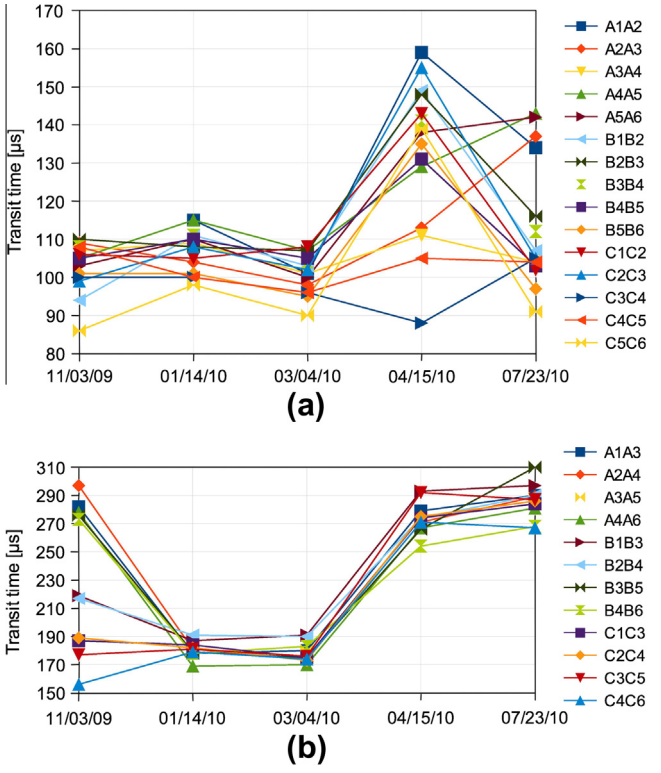


**Fig. 8.** Transverse transit times records for (a) 30 cm and (b) 60 cm spaced grid points.

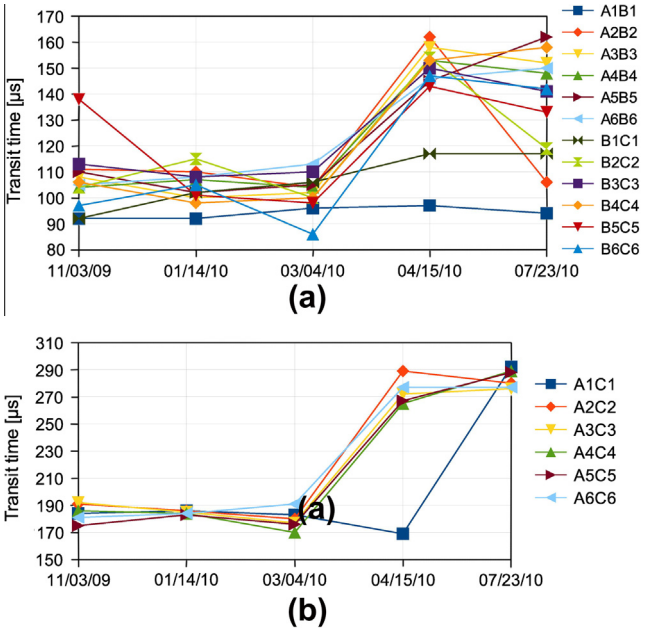


**Fig. 9.** Longitudinal transit times records for (a) 30 cm and (b) 60 cm spaced grid points.

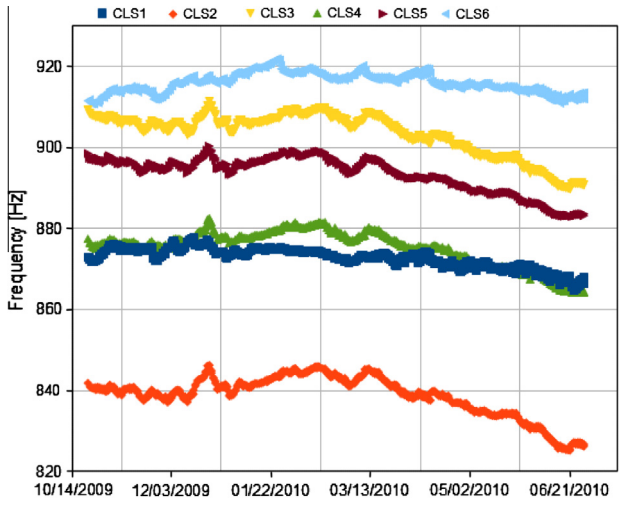


**Fig. 10.** Frequency values recorded by the embedment vibrating string gauges (CLS).

$$\Delta\varepsilon = G_f \times (f_2^2 - f_1^2); \tag{5}$$

where $f_1$ and $f_2$ are the reference and the actual vibrating frequencies of the string [Hz] and $G_f$ denotes the gauge factor, here equal to $3.304 \times 10^{-3}$ and $4.062 \times 10^{-3}$ respectively for embedment and arc weldable sensors. Frequency data from embedment sensors are gathered in Fig. 10.

They show a slow and negligible strain relaxation in both the longitudinal and transverse direction.

Similar results appear in Fig. 11, where arc weldable data are presented. Here, the strain reduction does not exceeds 3% of the original strain level and it is homogeneous for all gauges.

The recorded values of the pavement temperature furnished by the arc weldable sensors are reported in Fig. 12, the embedment gauges providing identical results. Note that only 5 series of temperature data have been reported in Fig. 12 because of a faulty connection between an arc weldable thermostat and the data logger.

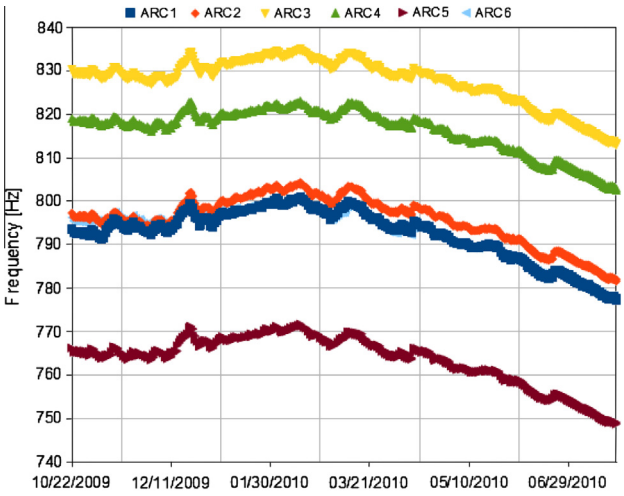


**Fig. 11.** Frequency values recorded by the arc-weldable vibrating string gauges (ARC).

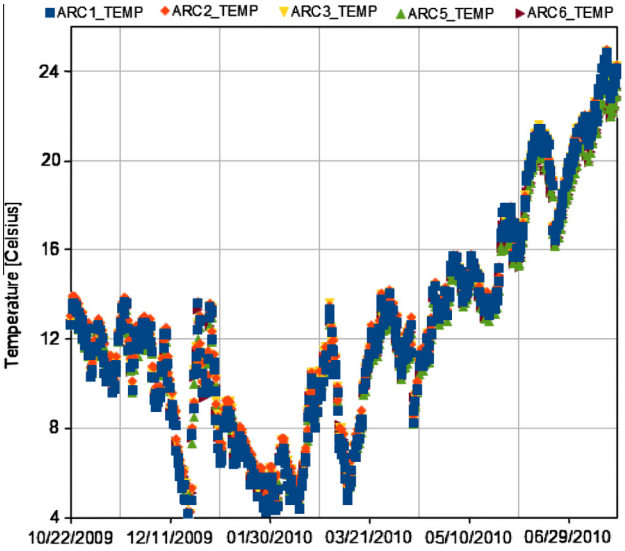


**Fig. 12.** Temperature values recorded by the arc weldable sensors.

Temperature fluctuations data may be positively checked against the transverse joint design width.

## 6. Conclusion

In this work, basic design guidelines for a polypropylene-based fiber reinforced concrete road pavement are presented. Such design was actually applied at a test section of the "Quadrilatero Marche-Umbria" road network empowerment project, Italy. Its main part lies in two major artificial tunnels, each about 30 km long, each carrying three lanes. The test road section is located in a secondary tunnel but it is meant to provide the testing ground for a full scale application of the technology in the main tunnel pavement.

To this aim, the design and construction stage is followed by a six month monitoring of the test section. Monitoring was carried out under actual traffic conditions, as the test section was opened to the public long before the full project was developed, taking advantage of the pre-existing road network.

The road condition is assessed through a continuous remote monitoring of the internal strain level, both in the longitudinal and transverse directions, inside the bulk of the pavement as well

as at the connecting bars in one transverse joint. The reliable and cost-effective vibrating string sensor technology was employed for it proved resistant to the manufacturing stage as well as to the heavy working conditions. Temperature compensation was envisaged.

The road surface condition is assessed through a men operated acoustic measuring device (ACT). Since men operated acoustic measuring is a cost and time consuming task, only a four month period could be covered. However, measuring was taken in both the longitudinal and transverse direction at a prescribed measuring grid. Besides, a one-grid-step and a two-grid-step measurement is reported, which supposedly accounts for the pavement damaging and the underlying supporting layer damaging, respectively.

It is shown that strain levels in the pavement rest very near to the initial pre-service condition and they are fairly consistent in space and time. In particular, a beneficial strain relaxation effect seems to dominate the readings.

On the other hand, acoustic measurements exhibit marked fluctuations, mainly due to the time-discrete an man operated reading procedure. Fluctuations are especially evident in long range measurements, which are more affected by signal noise. Nonetheless, it may be argued that the heavy rain conditions at the time caused a supporting layer loss of bearing capacity. In fact, although the test section rests in a tunnel, this is sloping and short enough to be affected by the external weather conditions.

Still, the overall behavior of the pavement appears almost invariable in time and the monitoring results support the validity of this design scheme for a PFRC road pavement.

## Acknowledgements

V. Costantino of Grandi Lavori Fincosit S.p.A. construction corporation (Roma, Italy) and A. Finamore of CMC Group (Ravenna, Italy) are gratefully acknowledged for their support. Mrs. Lorena Gamberini and Mr. Mariano Salvadore are gratefully acknowledged for providing polymeric fibres.

## References

[1] Hansen W, Jensen E, Mohr P, Jensen K, Pane I, Mohamed A. Effects of higher strength and associated concrete properties on pavement performance. Final Technical Report Publication No. FHWA-RD-00-161, Federal Highway Administration; 2001.
[2] Mohr P, Hansen W, Jensen E, Pane I. Transport properties of concrete pavements with excellent long-term in-service performance. Cem Concr Res 2000;30:1903–10.
[3] Debaillon C, Carlson P, He Y, Schnell T, Aktan F. Updates to research on recommended minimum levels for pavement marking retroreflectivity to meet driver night visibility needs. Publication No. FHWa-HRt-07-059, Federal Highway Administration; 2007.
[4] Hannant DJ. Durability of cement sheets reinforced with polypropylene networks. Mag Concr Res 1983;35(125):197–204.
[5] Grilli A, Bocci M, Tarantino AM. Experimental investigation on fibre-reinforced cement-treated materials using reclaimed asphalt. Constr Build Mater 2013;38:491–6.
[6] Kalifa P, Menneteau F-DG, Quenard D. Spalling and pore pressure in HPC at high temperatures. Cem Concr Res 2000;30:1915–27.
[7] Kalifa P, Chéné G, Gallé C. High-temperature behaviour of HPC with polypropylene fibres from spalling to microstructure. Cem Concr Res 2001;31(10):1487–99.
[8] Lanzoni L, Nobili A, Tarantino AM. Performance evaluation of a polypropylene-based draw-wired fibre for concrete structures. Constr Build Mater 2012;28(1):798–806.
[9] Jordaan GJ. South African roads board. Users manual for the south african mechanistic pavement rehabilitation design method. Report Nr IR91/242, Department of Transport, Pretoria, South, Africa; 1993.
[10] De Beer M. South African roads board. The evaluation, analysis and rehabilitation design of roads. Report Nr IR93/296, Department of Transport, Pretoria, South, Africa; 1994.
[11] Molenaar AAA. Structural design of pavements. Part III: Design of flexible pavements.
[12] Chang D-Il, Chai WK. Flexural fracture and fatigue behavior of steel–fibre-reinforced concrete structures. Nucl Eng Des 1995;156:201–7.
[13] Naaman AE, Hammoud H. Fatigue characteristics of high performance fibre-reinforced concrete. Cem Concr Comp 1998;20:353–63.
[14] Mailhot T, Bissonnette B, Saucier F, Pigeon M. Flexural fatigue behavior of steel fibre reinforced concrete before and after cracking. Mater Struct 2001;34:351–9.
[15] Lee MK, Barr BIG. An overview of the fatigue behaviour of plain and fibre reinforced concrete. Cem Concr Comp 2004;26:299–305.
[16] Singh SP, Mohammadi Y, Madan SK. Flexural fatigue strength of steel fibrous concrete containing mixed steel fibres. J Zhejiang Univ-Sc A 2006;7(8):1329–35.
[17] Norme Tecniche per le Costruzioni, DM 14 Gennaio 2008 (In Italian).
[18] Concrete industrial ground floors. A guide to design and construction. Concrete Society Technical Report No. 34. 3rd ed.
[19] Pristov E, Dalton W, Likins G. Measurement of concrete thickness and detection of defects using ultrasound methods. In: Proceedings of the fifth highway geophysics – NDE conference: Charlotte, NC; 2008. p. 295–301.
[20] UNI EN 12504-4. Testing concrete – Part 4: Determination of ultrasonic pulse velocity (in Italian); 2005.
[21] ASTM C597-02. Standard test method for pulse velocity through concrete; 2003.
[22] UNI EN 12390-3. Testing hardened concrete. Compressive strength and test specimens (in Italian); 2003.
[23] UNI EN 197-1. Cemento – Parte 1: Composizione, specificazioni e criteri di conformità per cementi comuni (in Italian); 2011.
[24] UNI EN 12620. Aggregates for concrete; 2008.